

# Frequency Separation Model Based on Infinite-Impulse Response Filter Applied To Hybrid Power Generation Intended For Residential Sector

Safa Slouma\*, Sondes Skander-Mustapha\*\*‡, Ilhem Slama-Belkhdja\*, Mohamed Machmoum\*\*\*

\* Université de Tunis El Manar, Ecole Nationale d'Ingénieurs de Tunis, LR11ES15 Laboratoire de Systèmes Electriques, 1002, Tunis, Tunisie

\*\* Université de Carthage, Ecole Nationale d'Architecture et d'Urbanisme, 2026, Sidi Bou Said, Tunisie

\*\*\* Institute of Research on Electrical Energy of Nantes-Atlantique IREENA, Saint-Nazaire, France

(safa.slouma@enit.utm.tn, sondes.skander@enit.utm.tn, ilhem.slamabelkhdja@enit.utm.tn, machmoum-m@univ-nantes.fr)

‡ Corresponding Author; Sondes Skander-Mustapha, Postal address, Tel: +216 71 874 700, Fax: +216 71 872 729, sondes.skander@enit.utm.tn

*Received: 20.10.2019 Accepted: 09.01.2019*

**Abstract-** This paper presents an optimal energy management system by means of frequency separation control, applied to an autonomous hybrid power generation intended for residential sector. Studied system is integrating photovoltaic and wind energy systems as main sources, and fuel cell stack as an auxiliary source. This residential hybrid power system is also including battery to support fast and large power demand fluctuation in order to preserve the fuel cell reliability and to enhance its lifetime. The models of the photovoltaic, wind, battery, fuel cell systems and the control strategy are carried out under MATLAB/SIMULINK. To display the performance of the studied energy management system, many scenarios are designed, in which the wind speed, the irradiance intensity and the load demand change over time. Simulation results illustrate the efficiency of the considered energy management system. The proposed strategy is validated experimentally in a lab-scale prototype. Experimental results are then presented to confirm the whole system performance and to verify the proposed controller efficiency.

**Keywords** Energy management system, Frequency separation, Autonomous hybrid system, Fuel cell, Battery.

## 1. Introduction

Nowadays, the growth of renewable energy facilities, such as wind turbines, and solar power plants, has provoked an emergent attention for energy networks including the interconnection of Distributed Generation units (DGs) and loads. Indeed, DGs based on renewable energy are attracting more and more interest for their environmental friendly characteristics [1] [2]. In addition, microgrids can be considered as independent electric systems that can supply loads even in autonomous mode. In addition to their use for supplying large buildings, islands and distant areas, microgrids are used to increase power quality, efficiency and reliability in power networks more than conventional AC power distribution systems [3] [4].

In an other hand, combining wind energy sources and PV with fuel cell systems (FCs) [5], could be part of the solution for distributed energy production because of the seasonally and daily disparities in the weather parameter. But, to improve system performance in transient mode, FCs that have slow dynamic response must be coupled to another energy storage system. Batteries are a good candidate to assume the function of auxiliary devices in this system, as they present fast transient response in addition to high power density and efficiency [6]. Thus, a battery storage system is joined to the FC to supply the primary power peak in case of transient operation, as load start-up, or sudden changes. The battery is also useful to cover the shortfall of generation system. Considering the problem of extending the FC lifetime, researchers are motivated by this idea and have presented several solutions to prolong FC lifetime. Indeed, many of the degradation methods have been proposed in the

literature, which are strongly affected by the FC functioning conditions and therefore can be reduced by the optimization of the energy management system (EMS). Furthermore, cooperative control strategy for FC based hybrid source has also been applied to estimate the effect of the energy management system on the FC degradation [7]-[11]. For example, in [7], Zhuol et al. shed light on an energy based optimization framework algorithm for FC and a battery system. This algorithm regulate the fuel flow rate simultaneously, and judiciously scales the load current to reduce the energy losses of the microgrid. This approach was employed to extend the lifetime of the used FC. Thounthong et al. [8] presented a FC Supercapacitor (SC) control strategy for electric vehicle application in which FC is functioning in steady state conditions. This approach was employed to reduce the FC mechanical stresses and to guarantee a best synchronization among FC current and fuel flow. Supercapacitors are used to cover transient power recoveries or deliveries. Accordingly, this strategy preserves the FC lifetime. Duarte et al. [9] include a particular bidirectional power converter in the hybrid FC battery system in order to improve power flow control and then improve FC lifetime.

For the autonomous operation of hybrid renewable electrical systems, Dufo-Lopez et al. [10], use genetic algorithms, to control autonomous microgrid based on renewable systems and including FC system and hydrogen storage. This approach minimizes the total cost throughout FC lifetime. In [11], a FC /battery power system was proposed, they are connected to the voltage bus via an hybrid full-bridge unidirectional converter and a three-level bidirectional converter, respectively. Fletcher et al. [12] investigated for a low speed vehicle control system by means of stochastic dynamic programming. The controller intends to minimize the total running cost of FC, the control allows to avoid FC transient loading to increase its lifetime. Thangavelautham et al. [13] propose to use filtering electronics to isolate fuel cell from electrical noise and power surge.

In this context, this work focuses on an autonomous hybrid system EMS based on the frequency control for residential use, applying DC load's fluctuating power allocation among the battery and FCs. This technique permits mitigating DC load's power fluctuations impacts for FCs and the residential microgrid. The key idea is to enlarge FC lifetime and minimize the stand-alone system cost. This approach has been mainly considered in the literature for marine and electric vehicles applications but has not been reported for residential sector for such hybrid system.

Furthermore, the work contribution consists of a control strategy based on infinite-impulse response (IIR) filter design according to availability and dynamic response of hybrid power generation systems. Several types of filters have been proposed in the literature for EMS based on frequency separation technique. For example, in [14] authors proposed an embedding adaptive frequency splitting for battery storage element coordinated with a supercapacitor (SC) energy management system control, where the adaptation approach of the filter frequency is determined according to the SC state of charge and the load current sign were also considered. In [15] authors study the case of fuel cell-battery hybrid electric vehicle. Therefore, a frequency splitter filter is used to orient

the power demand low frequency component towards the FC, to increase the life time of FC when load current sudden changes. The filter cut-off frequency is selected to smooth the FC response. In [16] frequency-separation strategy is adopted to direct the power demand low-frequency component towards the battery and its high frequency component towards the SC in order to preserve the battery life. In this paper, a frequency splitter (crossover) was proposed; the frequency can varied in real time to regulate the sharing among the SC and the battery power demands.

In clear contrast with the previously proposed methods, digital filter proposed in this work provides excellent advantages, such as better stability and precision. The major reason of the allocation of frequency between two components high and low frequencies is to reduce the effect of the microcycles caused by the DC load fluctuation.

This paper is structured as follows: Section 2 exposes a dynamic model of the proposed microgrid. In section 3 the system control based on frequency separation is discussed. After that the section 4 focuses on EMS of a stand-alone PV-WECS-FC system to supply the load requirements. Then, in section 5, experimental results are analyzed through an experimental test bench to illustrate the proposed EMS efficiency.

## 2. System description

Studied system is a DC hybrid system (Fig. 1). This system presents a developed model for distributed generation and offers important advantages: 1) optimization of system function [17]; 2) important ecological profit thanks to low emission generators [18]; 3) increasing the overall energy system efficiency [19]. The proposed DC hybrid system is designed to supply residential DC load.

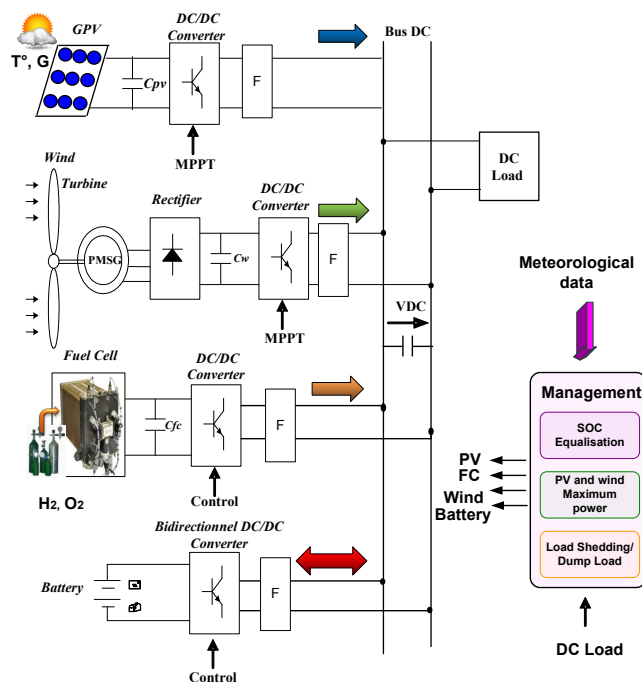


Fig. 1. Standalone DC microgrid configuration.

It consists of photovoltaic system connected to DC bus through a DC/DC converter, in addition to a wind turbine

based on a permanent magnet synchronous generator connected to the DC bus via a diode rectifier associated to a DC/DC converter which is controlled to achieve MPPT. Standalone DC microgrid incorporates also a Proton Exchange Membrane Fuel Cell integrated with batteries as storage devices, both are connected to the DC bus via a DC/DC converters, A management algorithm based on frequency separation control coordinates the overall functioning of the system.

2.1. Photovoltaic system

The studied PV cell model is shown in Fig. 2. Light current source  $I_{ph}$  is in parallel with a shunt resistance  $R_{sh}$  and a diode  $D_p$ . With a cell series resistance  $R_s$ .

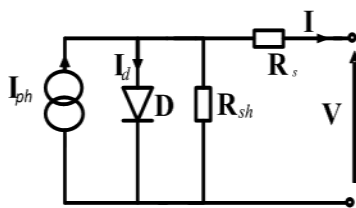


Fig. 2. PV cell Model.

Table 1 PV panels parameters

Maximum Power	85 Wp
Optimal Current	4.8 A
Optimal Voltage	17.8 V
Short circuit current	5.15 A
Open circuit Voltage	22.2 V

2.2. Wind generation system

The studied wind system, presented in Fig. 1 is based on a permanent magnet synchronous generator (PMSG). power electronic is composed of a three phase diode rectifier coupled to a controlled DC converter. to extract available wind maximum power. The PMSG parameters are given in Table 2.

Table 2 PMSG parameters

Average power (kW)	0.8
Number of poles	14
Stator resistance ( $\Omega$ )	0.5
Magnetizing rotor flux (Wb)	0.10402
Stator inductance (mH)	3.35

2.3. Energy Storage System

The adopted model of used battery is composed of a controlled voltage source connected with a constant

resistance. The battery is connected to the DC bus through a bi-directional DC/DC converter (Fig. 3). the control of the converter is based on two loops, the inner one controls the current and the outer one controls the voltage. In order to ensure DC bus voltage regulation under load steps.

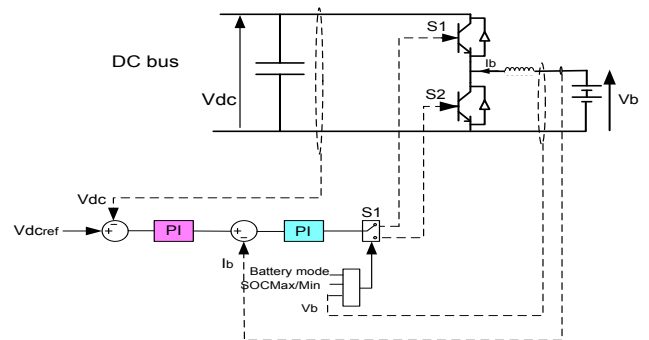


Fig. 3. Battery converter control.

2.4. Fuel cell system

The studied system include a Proton Exchange Membrane Fuel Cell this model is the most appropriate for residential appliance, it presents low operating temperature, high power density, efficiency and durability [20][21]

The FC performance is achieve by experimental test made in previous studies [22][23]. FC characteristic curves are established for a power of 155 W. FC stack includes 44 cells, the membrane active area is 16 cm<sup>2</sup> and air-hydrogen are supplied at the atmospheric pressure (1bar). The maximum current is 7 A.

The FC system is based on a DC-DC converter regulated with current control loop as exposed in (Fig. 4). The capacitor  $C_{fc}$  presents an overvoltage protection device acting when residential load causes high power transient. This FC control strategy not only minimizes fuel consumption, but also increases FC aging by reducing the FC current variation. Therefore, this control aims to deliver low frequency supplied by the FC through IIR filter design. Classical PI controllers are used that is able to regulate FC current  $I_{Lfc}$  to follow its reference  $I_{Lfc-ref}$ .

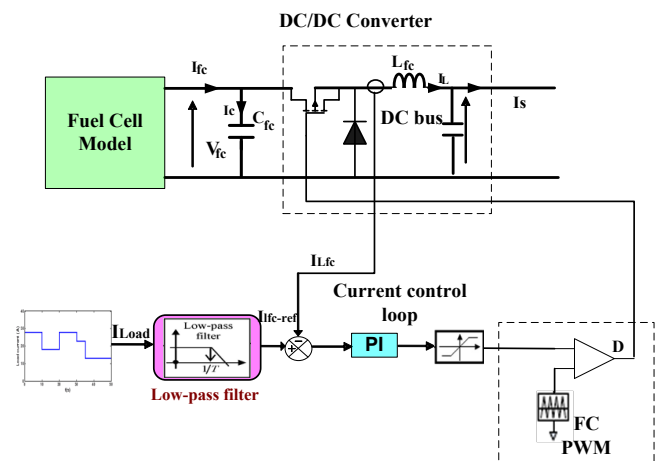
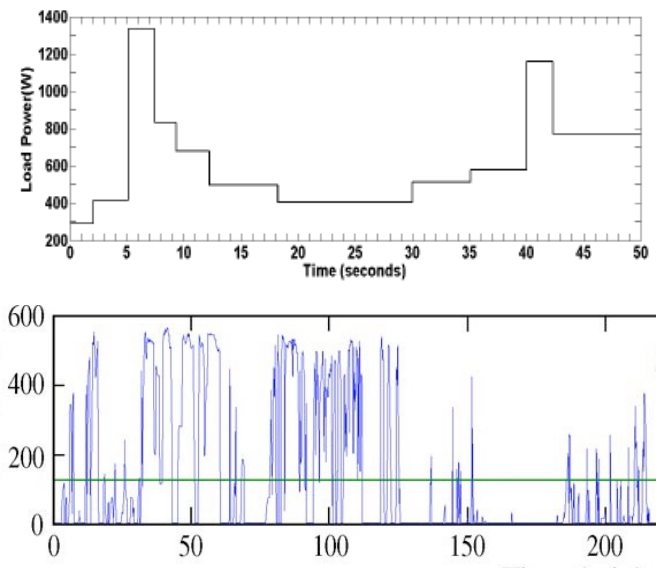


Fig. 4. Fuel cell control system.

### 2.5. Residential Load Profile

Each household appliance is characterized by a specific electrical profile with a steady and transient state conditions [24][25] [26]. Thereafter, two different load power profiles are presented: residential load [17] and vehicle [27] (Fig. 5). Indeed, Compared with an electric vehicle profile, step changing residential load power for steady, as well as transient cases is different. Since electric vehicle requires a considerably random and variable current due to transient traffic situations [28].



**Fig. 5.** Residential load power demand [17] and BB63000 Locomotive mission profile [27]

As home appliances present a switching on/off behavior which is observed by a peak value [24]. Control approach is tested with a rigorous load profile presenting a current rise hedge. Load current step variations are due to switching effects of residential units. Load current steps are applied at singular times: 10s, 20s, 30s and 35s (Fig. 6) to study the sources reaction when current peaks.

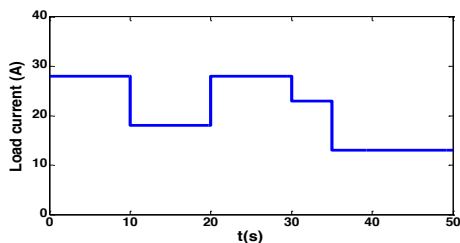


**Fig. 6.** Load current Profile.

### 3. Frequency separation control approach

The frequency separation control is applied to concretize the power frequency decomposition approach. Each source operates within its most suitable frequency range as high power density source or high energy density source. In the present study, this strategy is used to manage two special

types of power sources characterized by the FC as principal power source and a battery as an auxiliary source. FC is controlled to supply the mean power low-frequency, and battery is controlled to provide or to absorb the sudden variation of power demand.

A filter design cut-off frequency is fixed according to the FC characteristics and as depicted in Ragone plane [28] , in this study it varies from 10 mHz to 1Hz.

The proposed frequency separation strategy is exposed in (Fig. 7). In the considered approach, battery supplies the load power high frequency and huge power peak, while low frequency is directed to the FC. this results in a long-term autonomy. The power demand frequency decomposition is ensured through a cascade control.

The resulting power ( $P_{Load}-P_{PV}-P_W$ ) is filtered to achieve the BF Fuel cell power reference and the battery power reference presents the HF components.

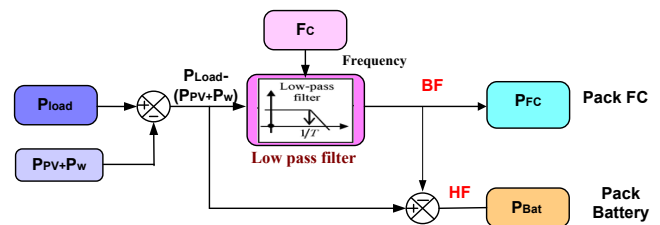


**Fig. 7.** Frequency separation control strategy.

Butterworth filter is chosen as a method of IIR filter synthesis. This filter choice is motivated as it is characterized by a flat frequency response curve with regular bandwidth amplitude, and easy calculations[30]. The recursive "Eq (1)" describes the direct form of the IIR filter [31]:

$$y(n) + \sum_{k=1}^M a_k y(n-k) = \sum_{k=0}^N b_k x(n-k) \quad (1)$$

Where  $x(n)$  are  $n^{th}$  system input and  $y(n)$  are  $n$  system output,  $N$  and  $M$  are numerator and denominator orders,  $a_k$  and  $b_k$  are IIR filter coefficients. After applying the Tustin transformation, transfer function of the IIR filter is as follows:

$$H(z^{-1}) = \frac{3.910^{-7} + 7.810^{-7} z^{-1} + 3.910^{-7} z^{-2}}{1 - 1.998z^{-1} + 0.998z^{-2}} \quad (2)$$

For the low-pass filter, a time constant must be used which corresponds to the FC operating ranges and the storage system. Indeed, the filter characteristics are calculated according to the FC parameters. Thus, it is necessary to begin by plotting the FC power curve as time function. Then we determine the cut-off frequency from these plotted curves. We suppose that  $\tau$  is the FC response time. Often, the time constant of the filter is fixed to  $3\tau$ . As for a safety measure, a time constant is fixed to  $5\tau$  in order to avoid the FC rapid aging [32].

Fig. 8 shows the FC power curve as time function. The simulation being carried out with a step, this curve shows that the FC response time corresponds to 0.2s. Therefore, the cut-off frequency considered will be 1Hz.

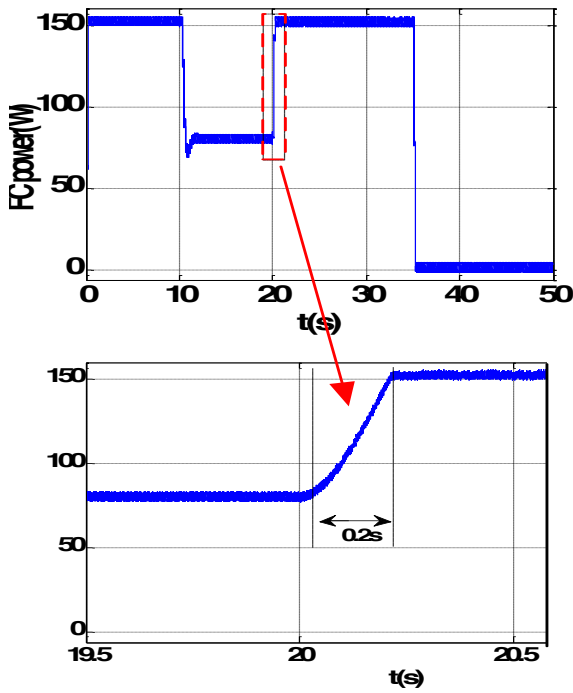


Fig. 8. FC power curve as time function.

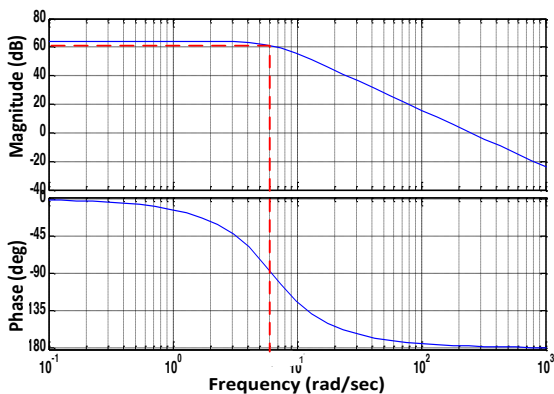


Fig. 9. IIR filter Bode Diagram.

Fig. 9 depicts the magnitude and dB responses of digital IIR filter designed. The characteristic frequency at -3 dB is equal to the cut-off frequency (1Hz).

The choice of separation frequency value is defined by the FC response time, guided by FC datasheet and the manufacturing technology. So, the filter time constant is chosen around few seconds.

#### 4. Energy Management System for hybrid system

The Energy Management System (EMS) permits to generate electric power. On the other hand, it allows the microgrid to guarantee load power constraints based on load profile, climatic conditions, objective function and constraints.

##### 4.1 Objective function

The power management aim is to satisfy load demand regardless of climatic conditions, ensure power equality between production and consumption “Eq.(3)”, as well as maximize PV and Wind sources production. The hybrid system power balance equation can be expressed as follows:

$$\sum_{a=1}^{N_{PV}} P_t^{PVa} + \sum_{b=1}^{N_W} P_t^{Wb} + P_t^{FC} + P_t^{Bat} = P_t^{Load} \quad (3)$$

Where  $N_{PV}$  is the PV panels number,  $N_W$  is the wind turbines number and  $P_t^{PV}$ ,  $P_t^W$ ,  $P_t^{FC}$ ,  $P_t^{Bat}$  ( $t$ ) are instantaneous power from PV, wind, FC, battery at time  $t$  respectively and  $P_t^{Load}$  is the instantaneous power demand at time  $t$ .

##### 4.2 Constraints

The EMS must guarantee that each component constraint is satisfied as the charging/discharging power limit in the study. On the other hand, to increase FC efficiency, it should operate at its maximum efficiency operating point, thus reducing fuel consumption. The following constraints shall be considered to extend FC life in the EMS and to minimize fuel consumption. The EMS is subject of the following constraints.

- Power Balance Constraints: deficit power system  
 The system can operate in energy deficit for a specified time interval “Eq.(4)”. So, the battery supplies the missing power to ensure load requirement. If load demand is not satisfied “Eq.(5)”, the fuel cell is activated to cover the energy shortage respecting the functioning within its maximum efficiency range. If the power system cannot supply the necessary load demand “Eq.(6)”, then non-priority loads are shedding.

$$P_t^W + P_t^{PV} < P_t^{Load} \quad (4)$$

$$P_t^W + P_t^{PV} + P_t^{Bat} < P_t^{Load} \quad (5)$$

$$P_t^W + P_t^{PV} + P_t^{FC} + P_t^{Bat} < P_t^{Load} \quad (6)$$

- Power Balance Constraints: surplus power system  
 If the maximum available power is greater than the power consumption “Eq.(7)”, then the extra power is directed to battery charging. When the SOC of the battery attains  $SOC_{max}$ , the surplus of the energy can be evacuated to the dump load.

$$P_t^W + P_t^{PV} > P_t^{Load} \quad (7)$$

##### 4.3 Algorithm

The proposed system power distribution algorithm is synthesized in Fig. 10. Based on weather conditions, objective function and constraints, the system power is calculated. The following modes have been investigated for the proposed algorithm:

- Charged battery Mode  
 If the maximum available power from the WECS and PV is larger than load demand with a battery capability to be

charged ( $SOC_t < SOC_{max}$ ), the surplus power  $P^{DL}$  can be stored in the battery :

$$P_t^{DL} = (P_t^W + P_t^{PV}) - P_t^{Load} \quad (8)$$

- **Dump load activated Mode**  
 The dump load function continues operating to ensure safe operating limits for the EMS. If the maximum power generated by Wind and PV is larger than load demand with a full charged battery,  $SOC_t \geq SOC_{max}$ , the surplus power can be supplied to a dump load, (electric water heater).

- **Discharging battery Mode**  
 In cases that the total power generated by wind and PV is lower than load demand, and also  $SOC_t \geq SOC_{min}$  ( $SOC_{min} = 40\%$ ); the battery can be used to meet load. The following equation expressed this mode:

$$P_t^{DL} = (P_t^W + P_t^{PV}) - P_t^{Load} \quad (9)$$

- **Fuel cell activated Mode**  
 If the summation of the power produced by PV, wind turbine and battery is less than load demand, FC needs to be activated to supply load demand
- **Fuel cell deactivated Mode**  
 If FC activation engenders a surplus power, then FC should be deactivated. The following "Eq.(10)" is investigated in this mode:

$$P_t^W + P_t^{PV} + P_t^{FC} + P_t^{Bat} > P_t^{Load} \quad (10)$$

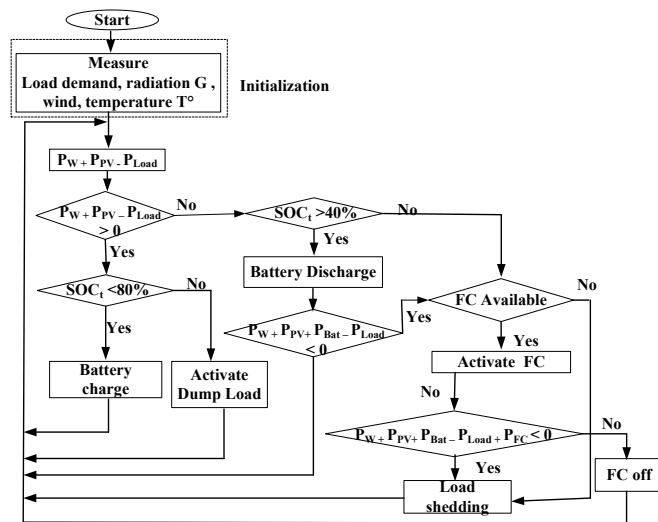


Fig. 10. Autonomous microgrid energy management algorithm

4.4 Simulation results

In the simulation, the test is performed with a load step variation at (2.6A to 5.1A).

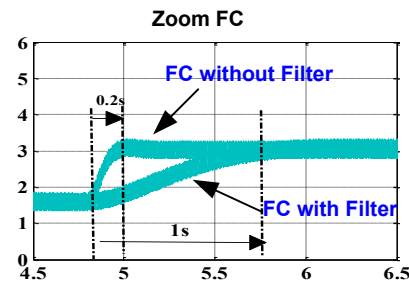
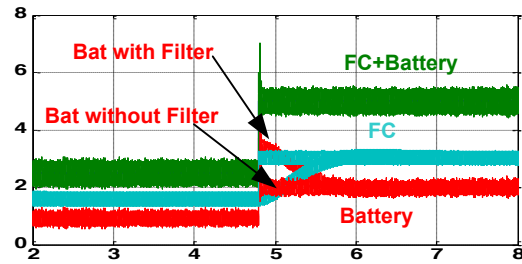


Fig. 11 presents the current allocation according to the planned percentages, 60% from FC and 40% from battery. The results highlight the decoupling method design; the objective to allocate the low frequency component to the FC and the high frequency transitions to the battery is attained. In fact, this method will enhance the FC performance by extending its lifetime. Furthermore,

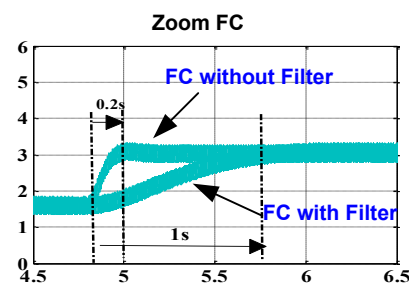
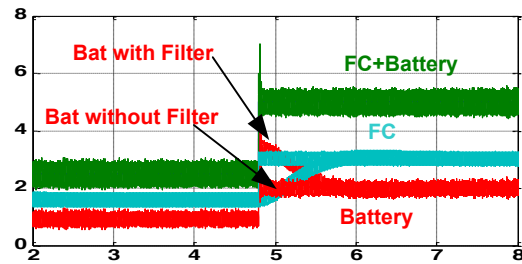


Fig. 11 shows that the sum of the sources current (FC and Battery) is equal the load current request. This result emphasizes the FC response time which is 0.2s as well as the precaution that the filter ensures by starting the FC at 1 s. It proves also the good design of the IIR filter for the separation frequency method.

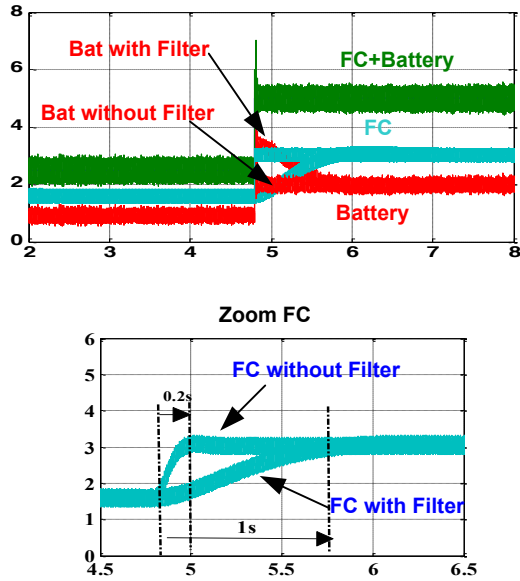


Fig. 11. FC and battery current responses through IIR filter for load step variation (from 2.6 A to 5.1 A).

To verify the proposed hybrid system performance, the total EMS has been validated in MATLAB/SIMUINK. The results obtained are exposed in Fig. 12, Fig. 13 and Fig. 14. The simulation results illustrate the current output variation of different sources in addition to load current, the whole generated current and DC bus voltage response.

Fig. 12 (a) shows the WT is generating 245 W at 6m/s. It is clear that the maximum WT power matches the WT produced power, which verifies that the MPPT imposes WECS to extract its maximum power. So the MPPT efficient of WEC system is validated.

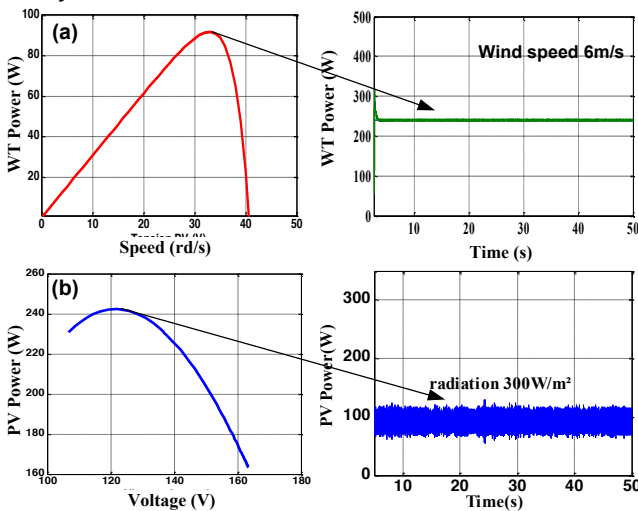


Fig. 12. Power produced by Wind Turbine (a) and PV (b).

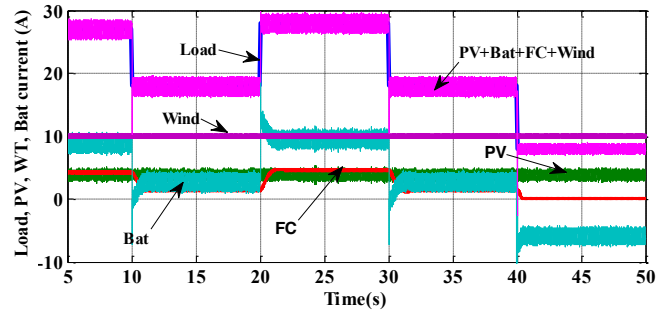


Fig. 13. Load, PV, Wind Turbine, Battery and Fuel cell current responses for several load steps.

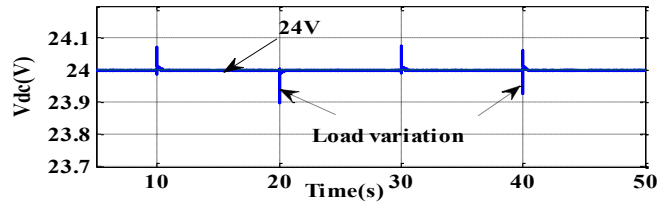


Fig. 14. DC bus voltage response for several load steps (voltage reference value = 24V)

Fig. 12 (b) shows that PVs generates 100 W<sub>p</sub> at 300 W/m<sup>2</sup>. It indicates that the maximum PV power matches with the produced power, which confirmed that the MPPT guides the PV systems to extract its maximum power. Results of simulation validate the PV MPPT and dynamic performance.

Fig. 13 shows the PVs, WECS, battery and fuel cell current change in concordance with load current deviation and start-up process. In these intervals [0s, 10s], [10s, 15s], [15s, 20s], [20s, 30s] and [30s, 40s], PVs and WECS cannot satisfy load demand. So, the battery supplies the load deficiency. The FC and battery dynamic interaction regarding the variation in the load current (at t=10s, 20s and 30s) is shown. We observe that under any change of load demand, the battery consumes or provides the transient load current. Battery will supply it immediately and FC will deliver its current with slow response (1s). At time 40s, the battery will absorb the transient current from load step. After satisfying the load demand The surplus energy is directed to charge the battery, as to the FC is deactivated.

Fig. 14 presents the DC bus voltage response when load current varies. It's clear that *V<sub>dc</sub>* follows well its reference (24V).

Simulation results illustrate the generated power supply reliability and its good performance in case of variable load according to user-configured frequency-separation algorithm.

### 5. Experimental results

To validate the proposed control algorithm, an experimental small scale test bench is accomplished (Fig. 15.). The test setup was built using fuel cell and battery emulators, an inverter, a variable load, two DC/DC power converters and a system controller. A DSP TMS32F-Discovery is utilized as a main controller. Fig. 16 illustrates the hybrid system hardware prototype.

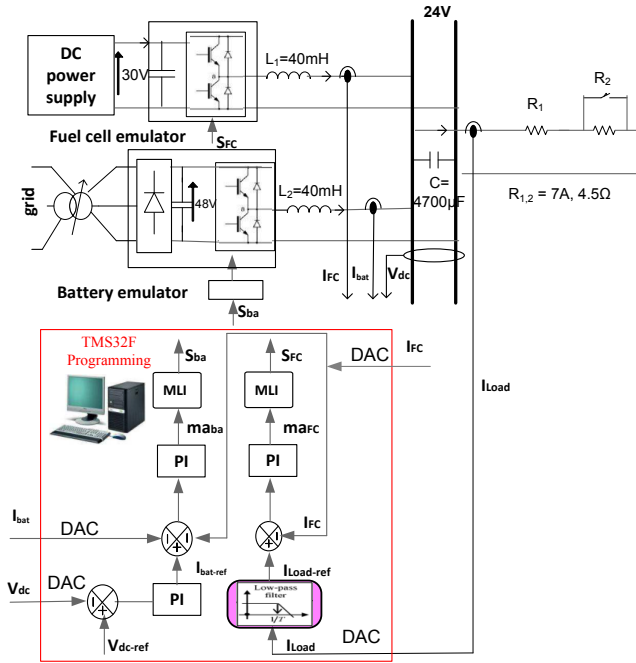


Fig. 15. Block diagram of the experimental setup with Control management strategy.

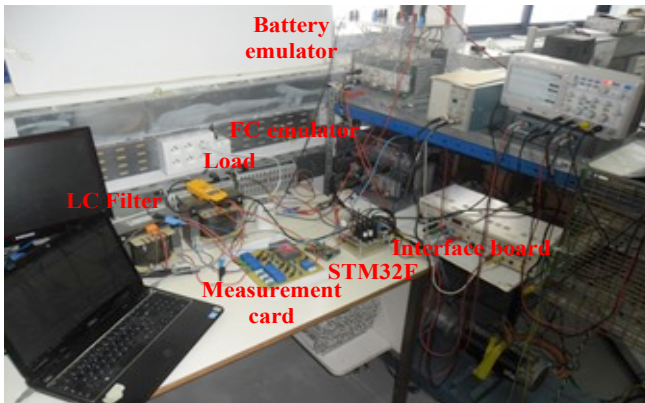


Fig. 16. Test bench picture.

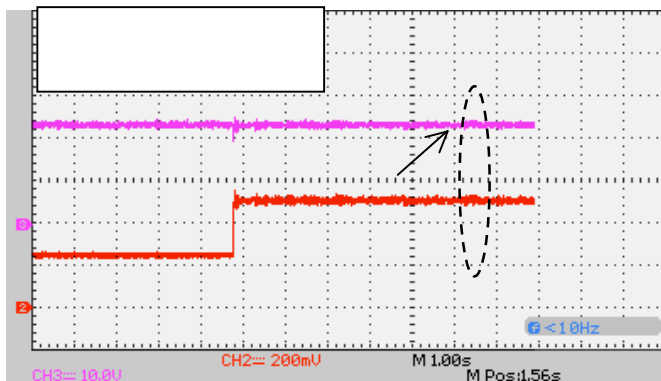
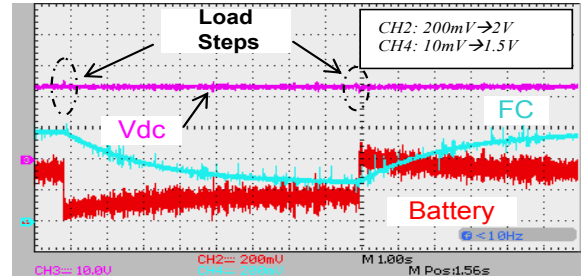


Fig. 17. (a) DC Bus voltage (10V/ Div) (b) Load step current from 2.6A to 5.1A (2A/200mV).

DC bus voltage reference value is fixed at 24V. To test the response of different used sources to current peaks, a load

current step is applied using frequency separation control. PI regulators are implemented to control the DC bus voltage ( $V_{dc}$ ), and the battery/FC currents. Initially, the study is focused on the battery/FC transient response under load steps. It consists on two loads current steps from 5.1 A to 2.6A, then from 2.6 A to 5.1 A as reported in Fig. 17.



Fi

g. 18 exposes FC and battery current, in addition to DC bus voltage responses in the hybrid source setup. The FC/battery hybrid system response shows a smooth FC current behavior and a slowly increase or decrease of FC current after each load step. As to battery current, it ensures power balance.

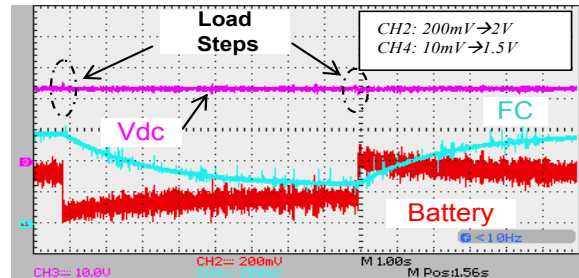


Fig.

18 depicts that DC bus voltage tracks well its reference (24V) with load current variations.

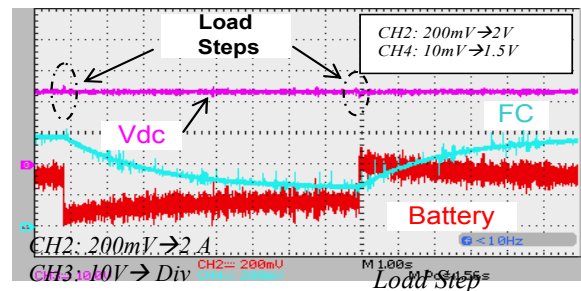
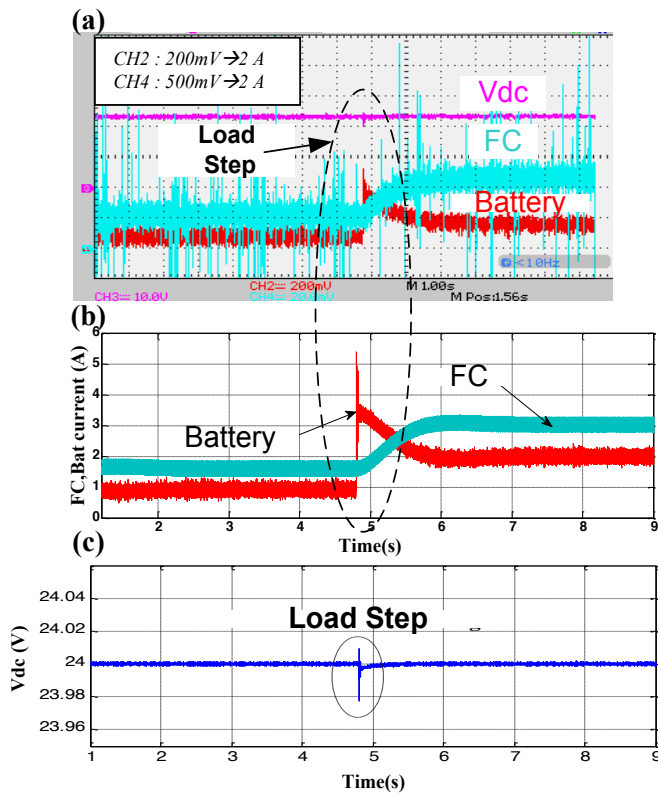


Fig.

18. DC bus voltage  $V_{dc}$  (pink), FC current (blue), Battery current (red) when load step.

$V_{dc}$   
 (b)  
 Load current





**Fig. 19.** The control strategy performance under load step. (a) experimental results: FC and Battery current responses under Load step from 2.6 to 5.1A. (b) and (c) simulation results

Fig. 19 (a) and (b) presents simulation and experimental system responses emphasizing the control performance, when the load current rises. The sudden increase of load current leads to a smoothly and slowly increase of fuel cell current, as to high frequency components which are depicted in the battery current. After load step, FC current rises slowly during 1 second in order to enlarge its lifetime. Note that the DC bus voltage follows its reference value (24V) (Fig. 19 (c)), as well as the control depicts a small overshoot at load step instant.

Experimental results are compared with that of the simulation ones (Fig. 19 (a) and Fig. 19 (b)), Indeed for both cases, the battery and FC currents are comparable in respect of response time: The battery supplies the load in transient operation, then FC supports slow variations of the charging current. the percentage of Battery/FC energy contributions is also respected and proved by experimental tests, which proves the efficiency of the proposed energy management approach.

## 6. Conclusion

This paper studies the optimal function of an hybrid renewable energy system. It presents a frequency separation strategy for hybrid system based on photovoltaic, wind and fuel cell systems designated to supply residential appliance. As domestic loads are typically characterized by a specific profile, hybrid system includes batteries used to support large and rapid load demand variations. an infinite-impulse

response low-pass filter is designed to assign load low-frequency to FC and high frequency to batteries. The main purpose of this strategy is to extend FC lifetime. An energy management system is performed with objectives to provide continuous load supply as well as to ensure system reliability, by avoiding transient currents supplied by the battery to protect FC.

Simulation results are accomplished and discussed showing the proposed control robustness. The considered system satisfies all the above-mentioned criteria. In addition, the DC link voltage remains steady through all system operations, ensuring an appropriate supply for load current load. Experimental results have been carried out with the developed test bench in order to confirm theoretical results achieved with separation frequency method.

## Acknowledgments

This work was supported by the Tunisian Ministry of High Education and Research under Grant LSE-ENIT-LR11ES15, and Institute of Research on Electrical Energy of Nantes Atlantique - IREENA, Saint-Nazaire, France.

## References

- [1] M.Tucci, S.Rivero, J. C. Vasquez, J. M. Guerrero and G. Ferrari-Trecate, "A Decentralized Scalable Approach to Voltage Control of DC Islanded Microgrids", IEEE Trans. Control Syst. Technol., DOI: 10.1109/TCST.2016.2525001, Vol. 24, no. 6, pp. 1965 – 1979, November 2016.
- [2] M. Saleh ; Y. Esa ; N. Onuorah ; A. A. Mohamed, "Optimal microgrids placement in electric distribution systems using complex network framework", IEEE 6th International Conference on Renewable Energy Research and Applications (ICRERA), pp. 1036 - 1040, November 2017
- [3] V. Nasirian, Q. Shafiee, J. M. Guerrero, F.L. Lewis and A. Davoudi, "Droop-Free Distributed Control for AC Microgrids", IEEE Trans. Power Electron., DOI: 10.1109/TPEL.2015.2414457, Vol. 31, no. 2, pp. 1600 – 1617, February 2016.
- [4] I. Keskin ; G. Soykan, "Reduction of peak power consumption by using photovoltaic panels in Turkey", IEEE 6th International Conference on Renewable Energy Research and Applications (ICRERA), pp. 886 - 890, November 2017
- [5] M. Chiandone ; C. Tam ; R. Campaner ; G. Sulligoi, "Electrical storage in distribution grids with renewable energy sources" IEEE 6th International Conference on Renewable Energy Research and Applications (ICRERA), pp. 880 - 885, November 2017
- [6] J. H. Ahn ; B. K. Lee , "A novel parallel control for modular energy storage system achieving high performance, redundancy and applicability", IEEE 6th International Conference on Renewable Energy Research and Applications (ICRERA), pp. 412 - 415, November 2017
- [7] J. Zhuol, C.Chakrabarti', N.Chang and S.Vrudhula, "Maximizing the Lifetime of Embedded Systems

- Powered by Fuel Cell-Battery Hybrids", 6th International Symposium on Low Power Electronics and Design (ISLPED), Tegernsee, Germany, pp.424-429, October 2006.
- [8] P.Thounthong , S.Rael and B.Davat, "Control strategy of fuel cell/supercapacitors hybrid power sources for electric vehicle", *J. Power Sources*, doi.org/10.1016/j.jpowsour.2005.09.014, Vol.158, pp. 806–814, 2006.
- [9] J.L. Duarte, M.Hendrix, and M.G.Simões, "Three-Port Bidirectional Converter for Hybrid Fuel Cell Systems"; *IEEE Trans. Power Electron.*, DOI: 10.1109/PESC.2004.1354836, Vol. 22, no. 2, pp. 480-487, March 2007.
- [10] R.D.Lopez, J.L. B.Agustina and J.Contrerasb, "Optimization of control strategies for stand-alone renewable energy systems with hydrogen storage", *Renewable Energy*, doi.org/10.1016/j.renene.2006.04.013 , Vol 32, pp 1102–1126, 2007.
- [11] K.Jin, X.Ruan, M.Yang and Min Xu, "A Hybrid Fuel Cell Power System ", *IEEE Trans. Ind. Electron.* DOI: 10.1109/TIE.2008.2008336, Vol. 56, no. 4, pp. 1212-1222, April 2009.
- [12] T.Fletcher, R.Thring and M.Watkinson, "An Energy Management Strategy to concurrently optimise fuel consumption & PEM fuel cell lifetime in a hybrid vehicle", *Int. J. Hydrogen Energy*, doi.org/10.1016/j.ijhydene.2016.08.157, Vol. 41, no 46, pp. 21503-21515, December 2016.
- [13] J.Thangavelautham, D. Gallardo, D.Strawser and S. Dubowsky, "Hybrid Fuel Cells Power for Long Duration Robot Missions in Field Environments", 14th International Conference on Climbing and Walking Robots and the Support Technologies for Mobile Machines, pp. 1-8, February 2017.
- [14] A. Florescu, S. Bacha, I. Munteanu, A.I. Bratcu, A. Rumeau, "Adaptive frequency-separation-based energy management system for electric vehicles", *J.Power Sources*, doi.org/10.1016/j.jpowsour.2015.01.117, Vol.280, pp.410-421, 2015.
- [15] H. Alloui, K. Marouani, M. Becherif, M. Nacer and M.E.H Benbouzid, "A Control Strategy Scheme for Fuel Cell-Vehicle Based on Frequency Separation", *International Conference on Green Energy (ICGE)*, DOI:10.1109/ICGE.2014.6835417, Sfax Tunisia, 25-27 March 2014 2014.
- [16] A. Florescu, S. Bacha, I. Munteanu, and A.I. Bratcu, "Frequency-Separation-Based Energy Management Control Strategy of Power Flows within Electric Vehicles using Ultracapacitors", 38th Annual Conference on IEEE Industrial Electronics Society, DOI: 10.1109/IECON.2012.6389426, Montréal, Canada pp.2957-2964, 25-28 October 2012.
- [17] I. Biswas, P. Bajpai, "Control of PV-FC-Battery-SC Hybrid System for Standalone DC load", *IEEE. Eighteenth National Power Systems Conference (NPSC)*, DOI: 10.1109/NPSC.2014.7103782, pp. 1 - 6, 18-20 December 2014.
- [18] Y.Guan, J.C. Vasquez and J. M. Guerrero, "Coordinated Secondary Control for Balanced Discharge Rate of Energy Storage System in Islanded AC Microgrids", *IEEE Trans. Ind. Appl.*, DOI: 10.1109/TIA.2016.2598724, Vol. 52, no. 6, , pp. 5019–5028, December 2016.
- [19] L. Meng, A. Luna, E. R. Díaz, B. Sun, T. Dragicevic, M. Savaghebi, J.C. Vasquez, J.M. Guerrero and AI, "System Integration and Advanced Hierarchical Control Architectures in the Microgrid Research Laboratory of Aalborg University", *IEEE Trans. Ind. Appl.*, DOI: 10.1109/TIA.2015.2504472, Vol. 52, no. 2, pp. 1736 - 1749, April 2016.
- [20] P.N. Papadopoulos, M. Kandyla, P. Kourtza, T.A. Papadopoulos, G.K. Papagiannis, "Parametric analysis of the steady state and dynamic performance of proton exchange membrane fuel cell models", *Renewable Energy*, doi.org/10.1016/j.renene.2014.05.010, Vol. 71, pp.23-31, 2014.
- [21] J. Kuo, C. Wang, "An integrated simulation model for PEM Fuel Cell power systems with a buck DC-DC converter", *Int. J. Hydrogen Energy*, doi.org/10.1016/j.ijhydene.2011.05.107, Vol. 36, No. 18, pp.11846–11855, 2011.
- [22] S. Slouma, S. Skander Mustapha, I. Slama Belkhdja, M.Orabi, "An improved simple Fuel Cell model for Energy Management in residential buildings", *J. Electrical Systems*, vol. 11, no 2, pp. 145 - 159, 2015.
- [23] S. Slouma, S. Skander Mustapha, I. Slama Belkhdja, M. Machmoum, "Frequency separation control of energy management system for building", 7th International Renewable Energy Congress (IREC), Tunisia, pp. 1 – 6, 2016.
- [24] F. Mouelhi, H. Ben Attia-Sethom, I. Slama-Belkhdja, L. Miègeville and P. Guérin, "A fast event detection algorithm for residential loads within normal and disturbed operating conditions", *Eur. J. Electr. Eng.*, vol. 18, no. 1-2, pp. 95 - 116, 2016.
- [25] Z. Wang and G. Zheng, "Residential Appliances Identification and Monitoring by a Non intrusive Method", *IEEE Transactions on Smart Grid*, DOI: 10.1109/TSG.2011.2163950, Vol. 3, No. 1,pp. 80 - 92. March 2012.
- [26] A. Kashani ; Y. Ozturk , Residential energy consumer behavior modification via gamification, *IEEE 6th International Conference on Renewable Energy Research and Applications (ICRERA)*, pp. 1221 - 1225, November 2017
- [27] A. Jaafar, C.R .Akli, B. Sareni, X. Roboam and A. Jeuness, "Sizing and Energy Management of a Hybrid Locomotive Based on Flywheel and Accumulators", *IEEE Trans.Vehicular Technology*, DOI: 10.1109/TVT.2009.2027328, Vol. 58, No. 8, pp. 3947-3958, October 2009.

- [28] B. Mebarki, B. Allaoua, B. Draoui, D. Belatrache  
“Study of the Energy Performance of a PEM Fuel Cell  
Vehicle”, INTERNATIONAL JOURNAL of  
RENEWABLE ENERGY RESEARCH, , vol. 7, no. 3,  
pp. 1395-1402, 2017.
- [29] S. J. Moura, J. B. Siegel, D. J. Siegel, H. K. Fathy,  
A. G. Stefanopoulou, “Education on Vehicle  
Electrification: Battery Systems, Fuel Cells, and  
Hydrogen”, IEEE VPPC-Vehicle Power and Propulsion  
Conference, DOI : 10.1109/VPPC.2010.5729150, Lille,  
France, pp.1-6, 1-3 September 2010.
- [30] A. Mohammadi, S.H. Zahiri, "Analysis of Swarm  
Intelligence and Evolutionary Computation Techniques  
in IIR Digital Filters Design", 1st Conference on Swarm  
Intelligence and Evolutionary Computation (CSIEC  
2016), Iran, , pp 64-69, 2016.
- [31] N. Agrawal, A. Kumar, and V. Bajaj, "Optimized  
Design of Digital IIR Filter using Artificial Bee Colony  
Algorithm ", International Conference on Signal  
Processing, Computing and Control (ISPCC), pp: 316-  
321, 2015.
- [32] W. Nwesaty, A. I. Bratcu, O. Sename, “MIMO H  
control for power source coordination: application to  
energy management systems of electric vehicles”, 19th  
International Federation of Automatic Control congress ,  
South Africa, pp. 24-29, August 2014.